



# COMPARATIVE ANALYSIS OF COCONUT HUSK AND LAMINATED PLASTIC PACKAGING CO-PYROLYSIS: RESPONSE SURFACE METHODOLOGY AND ARTIFICIAL NEURAL NETWORK APPROACH

Joselito A. Olalo and Aser N. Dino

Department of Mechanical Engineering, College of Engineering, Camarines Norte State College, Philippines

E-Mail: [joselito\\_olalo@yahoo.com](mailto:joselito_olalo@yahoo.com)

## ABSTRACT

The co-pyrolysis of plastic with biomass offers a promising solution to mitigate environmental health concerns associated with plastic waste. This technique has shown effectiveness in addressing waste issues by generating fuel oil from plastic and biomass waste. Many researchers have utilized pyrolysis technology, employing various optimization techniques to produce significant amounts of pyrolytic oil. This study aims to compare predictions of the percentage mass oil yield using an artificial neural network (ANN) and response surface methodology (RSM). Before the pyrolysis process, a 3k factorial Box-Behnken Design was employed to determine the number of experiments required. In RSM, a 2D contour plot illustrated the correlation of each parameter with the percentage oil yield. ANOVA analysis revealed the significance of the produced quadratic mathematical model, with a p-value below 0.05. Through the ANN modeling, the temperature, particle size, and the percentage of LPP were employed as the input, while two neurons were employed in 1 hidden layer. The resulting percentage oil yields were calculated, indicating a significant influence from temperature and the percentage of laminated plastic packaging. Simulation results from the ANN demonstrated strong agreement with a correlation coefficient of 99.5%, surpassing the 90.71% correlation coefficient observed in RSM. This underscores the advantage of using ANN for predictive modeling.

**Keywords:** coconut husk, LPP, RSM, ANN, co-pyrolysis.

Manuscript Received 21 April 2024; Revised 18 November 2024; Published 27 December 2024

## INTRODUCTION

In 2020, global plastic production reached approximately 367 million metric tons (Mt) [1]. With an anticipated 85% increase in the world's urban population by 2030 across both developed and developing nations, urbanization and population growth will lead to a substantial rise in plastic waste generation [2]. The escalating volume of residual waste, particularly non-recyclable laminated plastic packaging, poses a critical challenge in the country due to limited landfills and urban space constraints where most of this waste is generated. Illegally disposed waste, predominantly plastics, exacerbates marine pollution, leading to environmental degradation and harming marine life [3].

Various recycling methods, albeit labor-intensive, have been employed to reduce waste volumes in dumpsites [4]. Pyrolysis, one such method, converts waste into alternative fuel, yielding better output with lower NO<sub>x</sub> and SO<sub>x</sub> emissions upon combustion [5]. Co-pyrolysis of biomass and plastics can mitigate the adverse effects of plastics on human health and aid in energy recovery [6].

Agricultural waste, such as coconut husk, holds promise as an environmentally friendly resource due to its biodegradability [7]. The influence of process conditions on the pyrolysis of coconut husk, LPP, and their co-pyrolysis remains unknown.

Temperature significantly impacts pyrolytic oil yield, with higher temperatures promoting greater hydrocarbon production [8]. Different plastics degrade at various temperatures, affecting pyrolysis outcomes [9]. Particle size and residence time also influence oil yield and completion time in pyrolysis processes [10]. In terms of economic viability, pyrolysis offers lower operational costs and maintenance compared to market prices, with potential operational environmental benefits such as carbon credit generation [11]. Furthermore, pyrolysis contributes to reducing fossil usage and greenhouse gas emissions, making it a strategic tool in waste-to-energy conversion [12]. Although recycling is a method to alleviate plastic waste issues, the complexity and cost of waste separation make it labor-intensive [13]. Research focuses on discovering more efficient energy recovery processes from plastic waste, with pyrolysis emerging as a promising method due to its ability to thermally degrade plastics, reducing environmental problems associated with regular recycling treatments [14].

Response surface methodology is commonly employed to investigate the significant factors affected by different parameters [15], whereas modeling with artificial neural networks (ANNs) provides dependable and effective forecasts for intricate outcomes [16], [17].

In this research, response surface methodology and ANN are employed to examine the influence of temperature, particle size, and feedstock composition on



pyrolytic oil yield. Response surface methodology facilitates mathematical optimization, while ANN investigates correlations in co-pyrolysis conditions between coconut husk and waste plastic LPP concerning the percentage of oil yield.

## MATERIALS AND METHODS

### Work Plan

This study employed three main components. The first part (1) consisted of the batch co-pyrolysis runs. The second part (2) involved the utilization of response surface methodology. Lastly, the third part (3) entailed the analysis using artificial neural networks.

### Batch Co-Pyrolysis Runs



**Figure-1.** The coconut husk (CH) and laminated plastic packaging (LPP).

Batch experiments involving coconut husk and laminated plastic packaging were co-pyrolyzed under the parameters outlined in Table-1. Table-2 was generated using a 3k factorial Box-Behnken Design to minimize the required number of experiments.

**Table-1.** Parameters for batch pyrolysis runs.

| Temperatures °C | LPP-CH ratios (%) | Particle Sizes (cm) | Overall Residence Time (min) |
|-----------------|-------------------|---------------------|------------------------------|
| 500, 600, 700   | 68, 58, 49        | 1, 3, 5             | 10                           |

**Table-2.** Batch pyrolysis process conditions according to the Box-Behnken response surface design of the experiment.

| Run number      | Temperature (°C) | Particle size (cm) | Feedstock Composition (% LPP) |
|-----------------|------------------|--------------------|-------------------------------|
| 1               | 500              | 1                  | 58                            |
| 2               | 700              | 1                  | 58                            |
| 3               | 500              | 5                  | 58                            |
| 4               | 700              | 5                  | 58                            |
| 5               | 500              | 3                  | 68                            |
| 6               | 700              | 3                  | 68                            |
| 7               | 500              | 3                  | 49                            |
| 8               | 700              | 3                  | 49                            |
| 9               | 600              | 1                  | 68                            |
| 10              | 600              | 5                  | 68                            |
| 11              | 600              | 1                  | 49                            |
| 12              | 600              | 5                  | 49                            |
| 13 <sup>a</sup> | 600              | 3                  | 58                            |
| 14 <sup>a</sup> | 600              | 3                  | 58                            |
| 15 <sup>a</sup> | 600              | 3                  | 58                            |



The gases and volatile substances generated by the reactor were channeled into a condenser, where condensable materials underwent liquefaction as shown in Figure-2. Cold water flowing through the condenser facilitated its cooling and was collected. Upon completion of the designated residence time, the reactor was deactivated to allow for gradual cooling.

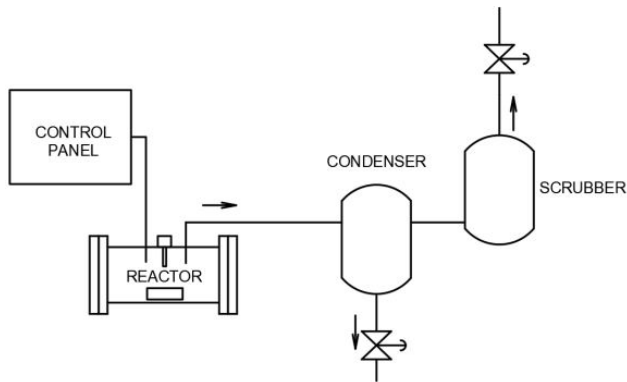


**Figure-2.** The pyrolysis system experimental set-up.

After the completion of pyrolysis, the oil obtained from the specified number of runs as detailed in Table-2 was utilized. Equation 1 was utilized to calculate the mass oil yield.

$$\%Yield = \frac{\text{weight of produced oil}}{\text{weight of feedstock}} \times 100 \% \quad (1)$$

### Response Surface Methodology

Table-2 displays the response parameters associated with temperature, particle size, and percentage feedstock composition for the pyrolysis of laminated plastic packaging. A 3k factorial Box-Behnken Design was utilized to determine the number of experimental runs, and ANOVA (Analysis-of-Variance) was employed to evaluate the significance of the predictive model in determining the percentage oil yield. Furthermore, a 2D-

contour plot was generated to illustrate the relationship between each response parameter.

### Artificial Neural Networks Analysis

The objective of artificial neural network analysis is to optimize and establish correlations between various input variables and the output variable in the percent oil yield. Utilizing Visual Gene Developer (VGD) 1.9 software, predicted values can be generated based on the available datasets. This software facilitates the construction of neural network structures and enables analysis and prediction mapping to determine the weights of each input variable.

The architecture of the artificial neural network utilized in this study follows a 3-2-1 feed-forward neural network (FFNN) model, employing a sigmoid activation function for each output neuron (refer to Figure-3). Creating the neural network required identifying the best combination of layers and neurons to achieve precise outcomes, a task frequently perceived as difficult [18].

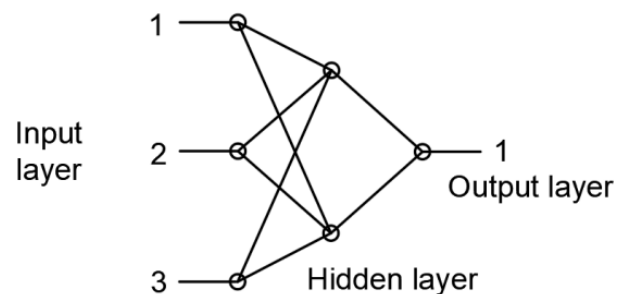


**Figure-3.** The input-hidden-output layers for the ANN model.

Before the training process, the datasets were normalized and the training process was initiated. This process entailed a maximum of 1 billion training cycles with a target error set at 0.00001.

**Table-3.** Actual percentage oil yield.

| Run number | Temperature (°C) | Particle size (cm) | Feedstock Composition (% LPP) | Actual Oil Yield (%) |
|------------|------------------|--------------------|-------------------------------|----------------------|
| 1          | 500              | 1                  | 58                            | 19.7                 |
| 2          | 700              | 1                  | 58                            | 25.0                 |
| 3          | 500              | 5                  | 58                            | 20.0                 |
| 4          | 700              | 5                  | 58                            | 30.5                 |
| 5          | 500              | 3                  | 68                            | 20.2                 |
| 6          | 700              | 3                  | 68                            | 25.5                 |
| 7          | 500              | 3                  | 49                            | 10.2                 |
| 8          | 700              | 3                  | 49                            | 25.2                 |
| 9          | 600              | 1                  | 68                            | 27.5                 |
| 10         | 600              | 5                  | 68                            | 31.2                 |
| 11         | 600              | 1                  | 49                            | 18.3                 |
| 12         | 600              | 5                  | 49                            | 14.0                 |
| 13         | 600              | 3                  | 58                            | 24.1                 |
| 14         | 600              | 3                  | 58                            | 23.4                 |
| 15         | 600              | 3                  | 58                            | 22.2                 |

## RESULTS AND DISCUSSIONS

### Percentage Oil Yield

Table-3 presents the percentage of oil yield for each individual run. The highest oil yield, reaching 31.2%, was observed at a temperature of 600°C, with a particle size of 5 cm and 68% LPP. This outcome was attributed to the combination of a larger particle size and a higher percentage of LPP. Conversely, the lowest oil yield recorded was 10.2%, occurring at a temperature of 500°C, with a particle size of 3 cm and 49% LPP. It is noted that an increased proportion of LPP tends to elevate the Oil yield.

In the co-pyrolysis of coconut husk and laminated plastic packaging, higher oil yields are observed at elevated temperatures at higher %LPP concentrations.

### ANOVA Results

The oil yield shows a consistent upward trend with increasing temperatures (within the experimental range of 500 - 700°C), while it demonstrates a decrease with a higher %CH concentration. While a weak positive correlation of 8.49% was observed between particle size to the percentage oil yield. The ANOVA results revealed a significant model with a P-value of 0.0386.

### Quadratic Mathematical Model to Predict Maximum Oil Yield

$$\begin{aligned}
 \text{Oil Yield (\%)} = & +7.52421 + (0.035046 * \text{temp}) - \\
 & (1.50941 * \text{particle size}) + (0.16677 * \\
 & \text{feedstock composition}) + [6.525\text{E} - 003 * \\
 & (\text{temperature. particle size})] + [2.5368\text{E} - 003 * \\
 & (\text{temperature. feedstock composition})] - [0.10553 * \\
 & (\text{particle size. feedstock composition}) - (9.5667\text{E} - \\
 & 005 * \text{temp}^2) + (0.38208 * \text{particle size}^2) - \\
 & (0.022345 * \text{feedstock composition}^2) ) \quad (2)
 \end{aligned}$$

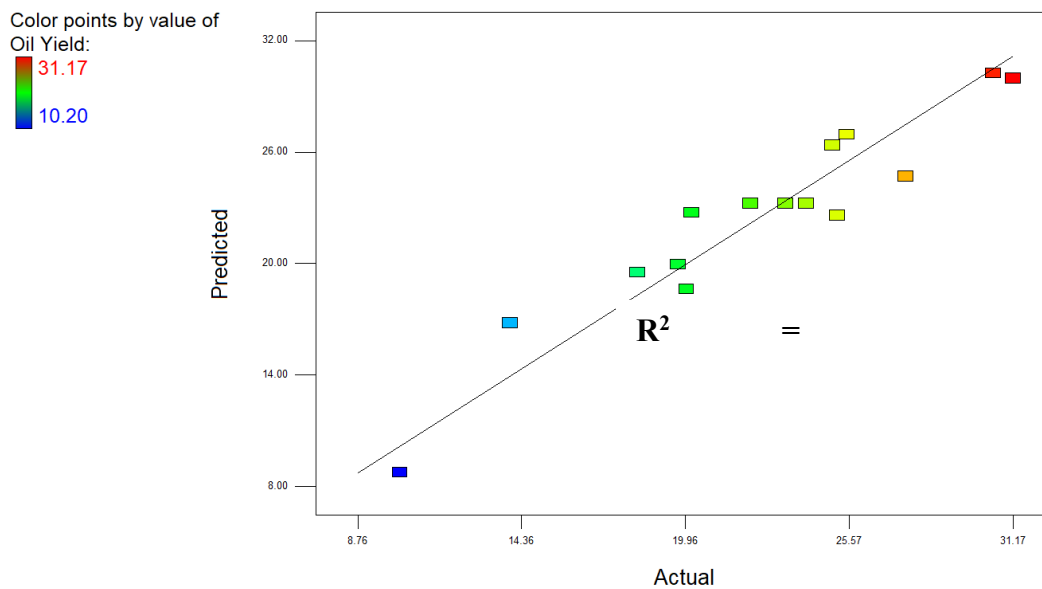
### Predicted Oil Yield via Response Surface Methodology

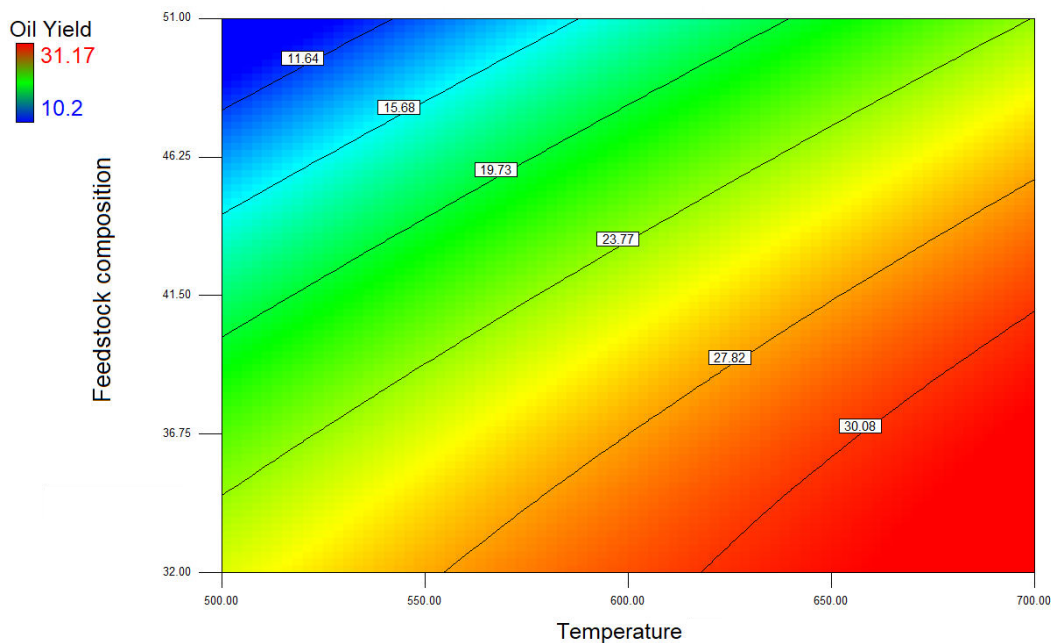
According to Table-4, the oil yield predicted using response surface methodology reached a maximum of 30.03% at a temperature of 700°C, a particle size of 5 cm, and a feedstock composition of 58% LPP. Conversely, the lowest oil yield of 8.76% was observed at a temperature of 500°C, a particle size of 3 cm, and a feedstock composition of 49% LPP.

Figure-3 depicts a correlation coefficient ( $R^2$ ) of approximately 90.71% between the predicted and actual percentage oil yield for coconut husk (CH) and laminated plastic packaging.

**Table-4.** Predicted percentage oil yield.

| Run number | Temperature (°C) | Particle size (cm) | Feedstock Composition (% LPP) | Predicted Oil Yield (%) |
|------------|------------------|--------------------|-------------------------------|-------------------------|
| 1          | 500              | 1                  | 58                            | 19.69                   |
| 2          | 700              | 1                  | 58                            | 26.36                   |
| 3          | 500              | 5                  | 58                            | 18.15                   |
| 4          | 700              | 5                  | 58                            | 30.03                   |
| 5          | 500              | 3                  | 68                            | 22.74                   |
| 6          | 700              | 3                  | 68                            | 26.94                   |
| 7          | 500              | 3                  | 49                            | 8.76                    |
| 8          | 700              | 3                  | 49                            | 22.6                    |
| 9          | 600              | 1                  | 68                            | 24.68                   |
| 10         | 600              | 5                  | 68                            | 29.97                   |
| 11         | 600              | 1                  | 49                            | 19.53                   |
| 12         | 600              | 5                  | 49                            | 16.79                   |
| 13         | 600              | 3                  | 58                            | 22.99                   |
| 14         | 600              | 3                  | 58                            | 22.99                   |
| 15         | 600              | 3                  | 58                            | 22.99                   |

**Figure-4.** Comparison of the predicted and actual values of oil yield for CH and laminated plastic packaging via RSM.



**Figure-5.** Two-dimensional contour plot of oil yield against temperature and feedstock composition.

Using 2D surface plots, the nature of the response surface and the adequacy of the model obtained for the effects of laminated plastic packaging were demonstrated. The 2D contour plots illustrated a classification of contour shapes for various applied parameters. It was observed that oil yield increased with temperature and decreased with the percentage feedstock composition of coconut husk (refer to Figure-5).

The highest oil yield, reaching 30.03%, was observed at 700°C with a 58% LPP feedstock composition, while the lowest oil yield, at 8.76%, was recorded at 500°C with a 49% LPP feedstock composition. Overall, there was a positive correlation between the percentage feedstock composition and temperature concerning oil yield.

#### Predicted Oil Yield via ANN

Figure-7 validates the efficiency of the model using a neural network between actual and predicted percentage oil yield. The results indicated a margin of error of  $\pm 0.12\%$  in the data obtained using the neural network. Utilizing VGD 1.9 software, it has achieved a sum of square error of  $\pm 0.00001$  with a correlation accuracy of 99.5%. While this level of accuracy is commendable, it is contingent upon the accuracy of the input data as well. The small margin of errors observed led to the actual percentage oil yield. This exemplifies how neural networks offer a viable solution for solving non-linear problems, providing an advantage over traditional statistical methods. The superiority of ANN modeling over statistical models is further justified as ANN establishes complex relationships between input and output variables, resulting in minimal prediction error, a feat not easily achievable through statistical methods [19].

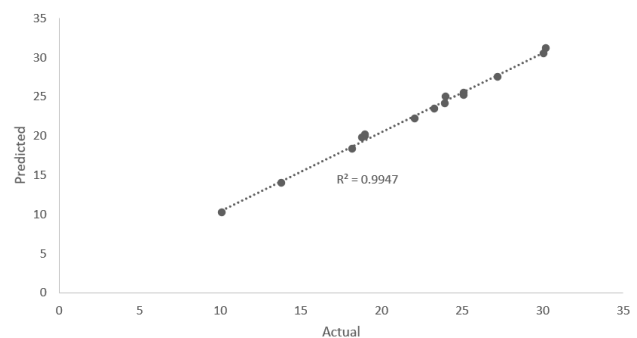


**Figure-6.** Actual versus predicted percentage oil yield via ANN.

The synaptic connections of the model encompass various weight values crucial for prediction. While the VGD 1.9 Software offers a neural network map analysis, as depicted in Figure-6. This diagram showcases the weights of the synapses connected to every neuron with the assistance of VGD 1.9 software. The legend indicates that near the "red" color, the weight value approaches a positive value, whereas near the "violet" color, the weight tends toward a negative value.

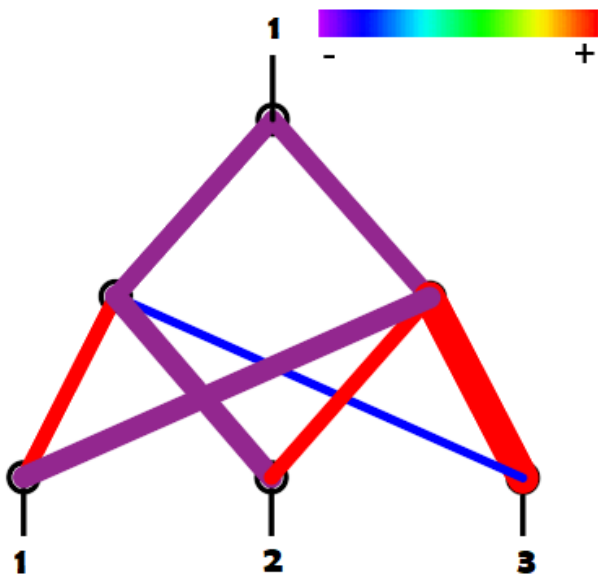


Figure-7. Neural network map analysis.

Table-5. ANN predicted the percentage of oil yield.

| Run number | Predicted Oil Yield (%) via ANN |
|------------|---------------------------------|
| 1          | 18.8                            |
| 2          | 24                              |
| 3          | 19                              |
| 4          | 30.05                           |
| 5          | 19                              |
| 6          | 25.1                            |
| 7          | 10.12                           |
| 8          | 25.1                            |
| 9          | 27.2                            |
| 10         | 30.2                            |
| 11         | 18.2                            |
| 12         | 13.8                            |
| 13         | 23.94                           |
| 14         | 23.3                            |
| 15         | 22.1                            |

It was observed in Table-5 that the optimum combination yielding the highest predicted oil yield of 30.2% corresponded to a temperature of 600°C, a particle size of 5 cm, and a 68 %LPP composition (as indicated in the corresponding Table-4). These values were obtained after de-normalizing the resulting predicted values using simulation in the artificial neural network.

## CONCLUSIONS

This study delved into the potential of using the co-pyrolysis method in producing liquid fuel from waste

laminated plastic packaging and coconut husk. The research aimed to explore the factors influencing a process and how the co-pyrolysis of these specific waste materials impacts the percentage of oil yield.

Two distinct methodologies were utilized to calculate correlation coefficients for the actual and predicted percentage oil yield. Response surface methodology (RSM) resulted in a correlation coefficient ( $R^2$ ) of 90.71 %, while artificial neural modeling (ANN) achieved an impressive  $R^2$  of 99.5 %, signifying high correlation accuracy that supports the increase in oil yield percentage. The ANN prediction model exhibited evident advantages, rendering it a more viable approach for addressing nonlinear problems.

## ACKNOWLEDGEMENT

The authors would like to thank Camarines Norte State College for the funding support of this research.

## REFERENCES

- [1] Plastics Europe. 2021. Plastics - the Facts 2021. An analysis of European plastics production, demand, and waste data. <https://plasticseurope.org/wp-content/uploads/2021/12/Plastics-the-Facts-2021-web-final.pdf> (Accessed 21 March 2024).
- [2] Chen Y., Awasthi A. K., Wei F., Tan Q. and Li J. 2021. Single-use plastics: production, usage, disposal, and adverse impacts. *Science of the Total Environment*. 752, 141772.
- [3] McGlade J. 2021. From Pollution to Solution: A Global Assessment of Marine Litter and Plastic Pollution. UN environment programme. ISBN: 978-92-807-3881-0.
- [4] Singh N., Hui D., Singh R., Ahuja I. P. S., Feo L. and Fraternali F. 2016. Recycling of plastic solid waste: a state-of-the-art review and future applications. *Composites. Part B* 115, 409-422.
- [5] Olalo J. 2022. Pyrolytic Oil Yield from Waste Plastic in Quezon City, Philippines: Optimization Using Response Surface Methodology. *International Journal of Renewable Energy Development*. 11(1): 325-332.
- [6] Caroko N., Saptoadi H. and Rohmat T. A. 2020. Heating Characteristics of Palm Oil Industry Solid Waste and Plastic Waste Mixture using a Microwave. *ASEAN Journal of Chemical Engineering*. 20(2), 174-183.
- [7] Melikoglu M., Ozdemir M. and Ates M. 2023. Pyrolysis kinetics, physicochemical characteristics



- and thermal decomposition behavior of agricultural wastes using thermogravimetric analysis. *Energy Nexus*. 11, 100231.
- [8] Al-Salem S. M. 2022. Slow pyrolysis of end-of-life tires (ELTs) grades: Effect of temperature on pyro-oil yield and quality. *Journal of Environmental Management*. 301, 113863.
- [9] Ahmad I., Khan M. I., Khan H., Ishaq M., Tariq R. and Gul K. 2014. Pyrolysis study of polypropylene and polyethylene into premium oil products. *International Journal of Green Energy*. 12, 663-71.
- [10] Pan R., Ferreira Martins M. and Debenest G. 2021. Pyrolysis of waste polyethylene in a semi-batch reactor to produce liquid fuel: Optimization of operating conditions. *Energy Conversion and Management*. 237, 114114.
- [11] Ayanoglu A. and Yumrutas R. 2016. Production of gasoline and diesel-like fuels from waste tire oil by using catalytic pyrolysis. *Energy*. 103, 456-468.
- [12] Benvenga M. A. C., Librantz A. F. H., Santana J. C. C. and Tambourgi E. B. 2016. A genetic algorithm was applied to study the economic viability of alcohol production from Cassava root from 2002 to 2013. *Journal of Cleaner Production*. 113, 483-494.
- [13] Peng Y., Wang Y., Ke L., Dai L., Wu Q., Cobb K., Zeng Y., Zou R., Liu Y. and Ruan R. 2022. A review on catalytic pyrolysis of plastic wastes to high-value products. *Energy Conversion and Management*. 115243.
- [14] Ford H. V., Jones N. H., Davies A. J., Godley B. J., Jambeck J. R., Napper I. E., Suckling C. C., Williams G. J., Woodall L. C. and Koldewey H. J. 2022. The fundamental links between climate change and marine plastic pollution. *Science of the Total Environment*. 806, 1-11.
- [15] Veza I., Spraggon M., Fattah I. M. R. and Iris M. 2023. Response surface methodology (RSM) for optimizing engine performance and emissions fueled with biofuel: a review of RSM for the sustainability energy transition. *Results in Engineering*. 18, 101213.
- [16] Olalo J. 2023. Exploring sustainable fuel production through thermal behavior analysis using TGA and artificial neural network in the co-pyrolysis of polystyrene and coconut sawmill residue. *ARPAN Journal of Engineering and Applied Sciences*. 18(23): 2540-2548.
- [17] Ospina-Alarcon M., Usuga-Manco L., Chanchi-Golondrino G. and Zapata-Cortes O. 2022. Neural network control design for an air pressure system. *ARPAN Journal of Engineering and Applied Sciences*. 17(13): 1323-1330.
- [18] Zhang M., Li P., Xia Y., Wang K. and Jin L. 2021. Labeling trick: a theory of using graph neural networks for multi-node representation learning. *Adv. Neural Inf. Process. Syst.* 34, 9061-9073.
- [19] Gupta R. K. and Singh R. C. 2024. Optimizing high-speed rotating shaft vibration control: Experimental investigation of squeeze film dampers and a comparative analysis using Artificial Neural Networks (ANN) and Response Surface Methodology (RSM). *Experts Systems with Applications*. 249(B): 123800.